BBA - Molecular Basis of Disease 1869 (2023) 166585

Contents lists available at ScienceDirect

BBA - Molecular Basis of Disease

journal homepage: www.elsevier.com/locate/bbadis

Vasoactive intestinal peptide deficiency promotes ovarian dysfunction associated to a proinflammatory microenvironment reminiscent of premature aging

Lucila Gallino [a], Vanesa Hauk [a], Lara Castagnola [a], Daiana Vota [a], Natalia Pascuali [b], Fernanda Parborell [b], Maria May [c], Vanina Fontana [a], Fatima Merech [a], Zaira Naguila [a], James Waschek [d], Claudia Perez Leirós [a], Rosanna Ramhorst [a,*]

[a] CONICET, Universidad de Buenos Aires, Instituto de Química Biológica de la Facultad de Ciencias Exactas y Naturales (IQUIBICEN), Buenos Aires, Argentina
[b] IBYME, CONICET, Buenos Aires, Argentina
[c] ININFA, Universidad de Buenos Aires, CONICET, Argentina
[d] The David Geffen School of Medicine, University of California, Los Angeles, USA

ARTICLE INFO

Keywords:
VIP
Ovary
Inflammation
Aging

ABSTRACT

Complex immune regulation during pregnancy is required to ensure a successful pregnancy outcome. Vasoactive intestinal peptide (VIP) has local immunoregulatory effects on the ovary, uterus and maternal-fetal interface that favor a tolerogenic maternal microenvironment. Since the VIP Knockout (KO) mice are subfertile, we investigated the mechanisms underlying the effects of VIP deficiency on ovarian physiology and immune homeostasis. Therefore, we studied VIP KO, deficient (HT) and wild type (WT) female mice in estrus at 3 or 8 months of age. Young KO mice showed abnormal cycle timing and regularity associated with dysfunctional ovaries. Ovaries presented higher number of atretic follicles and reduced number of corpora lutea leading to a lower ovulation rates. Part of the VIP KO mice (25 %) failed to ovulate or ovulated oocytes incompetent to be fertilized (50 %). In particular, ovaries of young KO mice exhibited features of premature aging accompanied by a pro-inflammatory milieu with increased levels of IL-1β. A unique macrophage subpopulation identified as "foamy macrophages" was found. On the other hand, aged VIP KO females did not gain body weight probably due to the sustained production of E2. Finally, the adoptive transfer of FOXP3+ cells to infertile VIP KO females resulted in their selective recruitment to the ovary. It increased FOXP3/RORγt and TGFβ/IL-6 ratio improving ovarian microenvironment and pregnancy rate. The present results suggest that VIP contributes to ovarian homeostatic mechanisms required for a successful pregnancy.

1. Introduction

Aging and reproductive potential in women are related and associated with the significant decrease in gamete quantity and quality [1]. Also, reproductive aging is associated with aneuploidy, miscarriages, birth defects and infertility, with a strong impact on maternal health [2]. In this sense, the ovarian microenvironment displays a significant impact on follicle and oocyte quality. Different cell populations such as fibroblasts, smooth muscle cells, endothelial cells, theca-interstitial cells and immune cells interact to sustain oocyte development.

In the last years, it was proposed the concept of "inflammaging" related to a chronic low-grade systemic inflammation that depends on age and is accompanied by increased levels of pro inflammatory cytokines [3–5]. This inflammatory microenvironment, characterized by IL-1β, IL-6, IL-8, and TNFα production as well as macrophages activation in a pro-inflammatory profile, may have a potentially detrimental impact on pregnancy. In fact, Duncan et al. described not only an increased expression of genes involved in inflammation, but also the presence of multinucleated macrophage giant cells [6]. However, the mechanisms underlying this phenomenon are not fully elucidated.

Abbreviations: VIP, vasoactive intestinal peptide; Tregs, regulatory T lymphocytes; E2, estradiol; P4, progesterone.

* Corresponding author at: Immunopharmacology Lab., School of Sciences, University of Buenos Aires, IQUIBICEN-CONICET, Int. Guiraldes 2160, Ciudad Universitaria, Pabellón 2 Piso 4, C1428EHA Buenos Aires, Argentina.
E-mail address: rramhorst@qb.fcen.uba.ar (R. Ramhorst).

https://doi.org/10.1016/j.bbadis.2022.166585
Received 7 March 2022; Received in revised form 15 October 2022; Accepted 20 October 2022
Available online 22 November 2022

On the other hand, regulatory T lymphocytes (Tregs, CD4 + FOXP3+ cells) are critical for controlling inflammation during the peri-implantation period and placentation. Several data obtained from *in vivo* and *in vitro* models demonstrate that Tregs are generated throughout gestation and are critical even before mating [7–10]. However, the immunoregulatory mechanisms that shape ovarian microenvironment during aging are still unknown as well as the role of macrophages and Tregs within the ovary.

VIP (vasoactive intestinal peptide) is a 28-amino acid basic peptide originally considered to be a gut hormone with vasodilatory action [11]. However, nowadays it is known that VIP expression is found in almost every tissue including the brain, endocrine tissues, respiratory system, digestive tract, intestinal tract, liver & gallbladder, pancreas, kidney & urinary bladder, male and female tissues, muscle tissues and bone marrow & lymphoid tissues (http://www.informatics.jax.org/marker/MGI:98933).

In 1976 it was demonstrated that VIP was localized in nerve fibers of both the central and peripheral nervous system [12]. Since then, its role in several physiological functions, acting in different organs including the genital tract and the ovary has been reported [13,14]. Particularly in the ovary, VIP is involved in many relevant processes as the regulation of the steroidogenic activity, estradiol and progesterone production in cultured granulosa cells [15–17]. VIP is an anti-inflammatory immunopeptide with immunoregulatory properties at the materno-placental interface. VIP is expressed by decidual and trophoblast cells displaying multiple effects shaping maternal leukocyte phenotype and function from decidualization to term [14,18–21].

VIP through VPAC1 and VPAC2 receptors coupled to adenylate cyclase conditions monocytes, dendritic cells and Tregs contributing to the selective recruitment of different immune cells during the peri-implantation period and the control of inflammation [18,19,22–26]. Accordingly, VIP knockout (KO) mice present a hostile environment for embryo implantation [23] along with an impaired trophoblast cell function at placentation and immune homeostasis loss [20,27–29]. VIP KO females are subfertile with longer intergestation periods and produce only half of the offspring of their WT female littermates [30]. Previous data support that VIP contributes to the selective recruitment of maternal Tregs toward the uterus. The adoptive transfer of CD4 + FOXP3+ improves uterine microenvironment allowing a successful implantation [23].

On the basis that aging affects the ovarian microenvironment associated to the induction of pro-inflammatory molecules expression, on one hand, and that VIP induces Treg cells which sustain tissue homeostasis by inducing anti-inflammatory and tolerogenic responses, here we explored the relevance of maternal VIP in ovarian immune regulation and its implication in premature aging. Using a VIP KO model, we analyzed the role of this immunopeptide *in vivo* as an endogenous regulator of the ovarian function to sustain immune homeostasis throughout the reproductive life. Whether VIP effects are associated to premature aging is also explored.

2. Materials and methods

2.1. Mouse models

Female VIP KO, HT, WT C57BL/6J [31], or FOXP3-IRES-GFP-knock-in [32] on a C57BL/6J background mice (3–8 months old) were bred and maintained in the Central Animal Care facility at the School of Sciences, University of Buenos Aires (FCEN-UBA). Briefly, VIP KO mice were obtained by targeting vector containing neomycin resistance and herpes simplex virus thymidine kinase genes was used to disrupt exon 4. The construct was electroporated in embryonic stem cells and injected into C57BL/6 blastocysts. On estrus day, animals were weighed with an analytical scale and then euthanized by CO_2 gas with confirmation by cervical dislocation at ZT1. Serum was extracted, and ovaries were weighed and stored on ice for future determinations. All studies were conducted according to standard protocols and were approved by the Animal Care and Use Committee of the School of Sciences, University of Buenos Aires.

The mice are housed in ventilated shelves model MACS of Alternative Design with air filtration system of inlet and exit by pre-filters and HEPA filters. Maximum 5 animals per box of stock (size 18.41 × 29.21 × 12.7 cm). Photoperiod of 12 h light and 12 h dark, experience rooms from 6 am to 6 pm, regulated by automatic digital clock switch.

2.2. Characterization of estrous cycles by vaginal lavage

WT (n = 5), VIP HT (n = 5), and VIP KO (n = 5) female mice (3 months old) housed under a 12:12 light–dark (LD) cycle were monitored to determine the estrous cycle using vaginal lavage at the same time of the day (ZT 1) for 14 consecutive days. Precaution was taken during the vaginal lavage to avoid any damage by the pipette, and the lavage samples were spotted in small (~100 μl) drops onto glass microscope slides. Cell types contained within each vaginal smear were determined using light microscopy (40×) and scored for estrus stage, where proestrus is indicated by the predominance of nucleated epithelial cells, estrus is denoted by the absence of nucleated cells and the presence of cornified squamous epithelial cells, and smears from mice in metestrus and diestrus contain leukocytes [33]. The cycle's length was measured as the average days from estrus to the next estrus from each animal during the 14 days. The percentage of proestrus smears followed by estrus were determined by scoring the number of proestrus smears that were immediately followed by an estrus smear compared with the total number of proestrus smears within each female. To determine the number of consecutive leukocyte smears, it was counted for each animal how many uninterrupted days they stayed in metestrus/diestrus during the two weeks.

2.3. Tissue collection

To obtain ovaries, uterus, implantation sites, and para-aortic lymph nodes, mice were euthanized by CO_2 gas with confirmation by cervical dislocation at ZT1. The skin abdomen was opened, the organs were identified, dissected out and placed in 10 ml of fresh cold media (Dulbecco's modified Eagle medium, DMEM F12, supplemented with 10 % fetal bovine serum). Excess fat and connective tissue were removed and each tissue was transfected into four to five donut-shaped pieces.

For flow cytometry assays, tissues were minced using a cell strainer [100 μm (BIOFIL)]. The cell suspension was centrifuged, the supernatant was discarded and the resultant cell pellet was taken for cell staining or sorting. For cytokine measurements, the pieces were cultured in 0.5 ml of media Dulbecco's modified Eagle medium (DMEM F12) supplemented with 10 % fetal bovine serum (FBS) in 24-well plates (Corning Glass, Corning, NY) for 48 h at 37 °C.

2.4. Embryo recovery, collection and culture

WT (n = 4) and VIP KO (n = 4) female mice (3 months old, average body weight of 23 g) were mated and, after 24 h, inspected for the presence of a vaginal plug. Those with positive vaginal plugs were euthanized by cervical dislocation at day 1.5 of gestation (day 0.5 = vaginal plug) at ZT1. The cells found in the oviducts were washed with pre-warmed PBS and kept at 37 °C in an atmosphere of 5 % CO_2 until seeding. Then, only the two-cell embryos were cultured for 72 h in 20 μL drops of pre-equilibrated Global Total medium (Life Global Group). At that point, the number of blastocysts was registered. Cultures were maintained at 37 °C in 5 % CO_2 in air.

2.5. IL-1β ELISA

After 48 h of culture at 37 °C, the ovaries were removed and the conditioned media centrifuged 15 min at 2000g. The supernatant was

stored at −20 °C until assayed. IL-1ß ELISA commercial kit (BD biosciences) was performed according to the manufacturer's recommendations.

2.6. Measurement of serum hormones

Serum was collected from 3-month-old WT ($n = 5$), HT (n = 5) and VIP KO (n = 5) female mice or 8-month-old WT (n = 5), HT (n = 5) and VIP KO (n = 5) female mice at ZT1 on the day of an estrus smear. To obtain serum, blood samples were allowed to clot at room temperature for 30 min prior to centrifugation at 3000*g* at room temperature. The supernatant was stored at −20 °C until assayed. Serum estradiol (E2) and progesterone (P4) concentration was determined using the ARCHITECT Estradiol assay (Ref 7K72) and the immulite 2000 Xpi Siemens Platform (Catalog Number: L2KPW2) respectively. The values were normalized to serum volume and expressed as pg/ml of serum for E2 and ng/ml of serum for P4. The estradiol assay precision is ≤5 pg/mL for concentrations in the range of 45 pg/mL, and ≤7 % for concentrations in the range of 190 pg/mL. The functional sensitivity of the estradiol assay is ≤25 pg/mL. The Progesterone assay precision is ≤0.1 ng/mL with a detection limit between 0.2 and 40 ng/ml. The intra-assay and inter-assay variations were 5 % and 6 % for E2 and 9.7 % and 10.5 % for P4.

2.7. Estradiol and progesterone determination by radioimmunoassay (RIA)

Steroid extraction from whole ovaries and their controls was performed as previously described [34,35]. Labelled steroids were added as internal standards during extraction, with a recovery percentage between 60 and 80 %. The final residues were resuspended in RIA buffer (Na2HPO4 40 mM; NaH2PO4 39.5 mM, NaCl 155 mM, sodium azide 0.1 %, gelatin 1 %, pH = 7.0) and stored at −20 °C until further analysis.

Ovarian estradiol (E2) and progesterone (P4) levels were measured by RIA in ovarian samples from 3-month-old WT ($n = 5$), HT (n = 5) and VIP KO (n = 5) female mice or 8-month-old WT (n = 5), HT (n = 5) and VIP KO (n = 5) female mice, as previously described [35,36]. Briefly, E2 and P4 concentrations in ovarian tissue were measured using specific antibodies supplied by Dr. G.D. Niswender (Animal Reproduction and Biotechnology Laboratory, Colorado State University, Fort Collins, CO, USA). The range of the assay using a final volume of 0.5 mL was 6.25–800 pg for E2 and 12.5–2000 pg for P4. Under these conditions, the intra-assay and interassay variations were 7.2 % and 12.5 % for E2 and 8.0 % and 14.2 % for P4. The values were normalized to protein content, as measured by the Bradford assay, and expressed as ng per mg of ovarian protein.

2.8. Ovarian morphology and follicle count

Mice ovaries were removed at ZT1 and then fixed in 4 % paraformaldehyde for 8 h at room temperature. The tissues were embedded in paraffin wax, sections of 5 μm were cut and placed on silanized glass slides and hematoxylin–eosin (H&E) staining was performed.

Ovarian sections (5 μm) were mounted at 50-μm intervals onto microscope slides to prevent counting the same structure twice, according to the method described by Woodruff et al. [37].

Primary, preantral, antral and atretic follicles, as well as corpora lutea (CL) were counted in ovaries from each experimental group. Randomly selected fields from each ovarian section were analyzed (3 sections/ovary, $n = 5$ ovaries/group). The total number of ovarian structures in each ovary (all follicle types + CL) was defined as 100 %. Data are expressed as the percentage of each type of structure per ovary.

A primary follicle was defined as an enlarged oocyte surrounded by a single layer of cuboidal granulosa cells. Oocytes with two or more layers of granulosa cells but no visible space between granulosa cells were identified as preantral follicles. Antral follicles were scored when containing several layers of granulosa cells, an oocyte with a clear nucleus, an antrum and a theca layer. Atretic follicles were counted only when a degenerating oocyte and pycnotic granulosa cells were observed. CL were defined as large structures that were primarily composed by polyhedric cells with central nuclei and that contained many lipid droplets. They differ from follicles in that the basal membrane is ruptured and the granulosa compartment has been invaded by connective tissue fibers and blood vessels, thus being a highly vascularized structure.

2.9. Flow cytometry analysis

For flow cytometry assays, tissues were minced using a cell strainer [100 μm (BIOFIL)], cell suspension was centrifuged and the resultant cell pellet analyzed. A CD4+ cell staining was performed from ovaries, uterus, implantation sites, para-aortic lymph nodes and spleen following manufacturer's instruction. Briefly, 1×10^6 cells were stained with anti-CD4 PE-conjugated (Becton Dickinson, San José, CA, United States). After 30 min, cells were washed, and 20,000 events were acquired in a fluorescence-activated cell sorting (FACS) FACS Aria II cytometer R (Becton Dickinson, San José, CA, United States). The results were analyzed using the FLOWJO 7.6.2 software. Negative control samples were incubated in parallel with an irrelevant, isotype-matched Ab. Results for positive cells were expressed as a percentage of the respective population and the quadrant was set using irrelevant isotype-specific mAb. Particularly for Treg analysis, FOXP3-positive cells were determined inside the electronically gated CD4-positive cell population.

For the adoptive cell transfer assays, GFP FOXP3+ cells were obtained from inguinal and mesenteric lymph nodes from GFP-knock-in mice at ZT1. The cell population that expressed the GFP marker was sorted using a FACS Aria II cytometer.

2.10. Adoptive cell transfer of Tregs

Two months of age VIP KO females were mated during 2 weeks with 3 months old WT males and, after that time, separated 2 more weeks to determine which females did not achieve pregnancy. To follow Treg *in vivo* migration, those females ($n = 3$) received an injection of 200,000 Tregs taken from the draining lymph nodes of a FOXP3-GFP-knock-in female 3 months old obtained by sorting as described before. Briefly, the lymph nodes were minced using a cell strainer (100 μm) and the cell suspension was centrifuged. The supernatant was discarded, the resultant cell pellet was resuspended in 0.3 ml of FACS and taken for sorting of FOXP3-GFP+ cells using a FACS Aria II cytometer R in sterile conditions. The purified Tregs (99 % purity) were washed twice with PBS and then resuspended in 0.2 ml of PBS and injected through the tail vein to the adopting mice at ZT5. The females were sacrificed 48 h later and CD4+ and GFP+ cells were quantified in ovaries, uterus, para-aortic lymph nodes and spleen. Ovaries were also evaluated by RT-PCR. In another set of experiments, females were mated again with the same male used previously. Vaginal plug was checked every day and, when found, animals were sacrificed at d5.5 at ZT1. Ovaries, implantation sites, para-aortic lymph nodes and spleen were pulverized through a 100 μm cell strainer, stained for anti CD4 and then analyzed by flow cytometry. Data are shown as % of GFP+ cells from the CD4+ population or as % of GFP+ cells from the 200,000 Treg cells injected.

2.11. FOXP3, RORγt and pro/anti-inflammatory mediators' detection

The expression of transcription factors and pro/anti-inflammatory mediators was determined by RT-PCR in the ovaries before and after the adoptive transfer of Tregs at ZT1. Briefly, total RNA was isolated following manufacturer's recommendations with Trizol reagent (Life Technologies, Grand Island, NY, USA), cDNAs were generated from 1 μg of RNA using a MMLV reverse transcriptase, RNAsin RNAse inhibitor and oligodT kit (Promega Corporation, Madison, WI, USA) and stored at −20 °C for batch analysis. The sample volume was increased to 25 μl with the solution containing 50 mM KCl; 10 mM Tris (pH 8.3); 1.5 mM

MgCl2; 0.1 mM forward and reverse primers of FOXP3, RORγT, TGF-β, IL-6 and GAPDH as internal control (described in Table 1) and 1 U Taq polymerase in a DNA Thermocycler (PerkinElmer/Cetus, Boston, MA, USA). PCR products were electrophoresed through a 2 % ethidium bromide-stained agarose gel, visualized by transillumination and scanned. Densitometry was performed using ImageJ 1.47 software (NIH, USA) and results expressed as arbitrary units normalized to GAPDH expression. Each assay included a DNA minus control and a standard curve performed with serial dilutions of control cDNA.

2.12. Statistical analysis

Data was analyzed using GraphPad Prism7 software (GraphPad, San Diego, CA, United States). For non-parametric analysis Kruskal Wallis test was used. One-way ANOVA with Dunn's multiple comparisons test, or two-way ANOVA with Tukey's multiple comparisons test were used for parametric analysis. A value of $p < 0.05$ was considered significant.

3. Results

3.1. VIP deficient females show irregular estrous cycles during reproductive age

On the knowledge that VIP KO females are subfertile and considering the effects of VIP at implantation and early pregnancy, we used VIP KO mice as an *in vivo* model to test the hypothesis that VIP has a role in the physiology of the immune response in the ovary. First, we evaluated if VIP deficiency disrupts the 4-day estrous cycle in VIP KO and HT females by daily examination of the vaginal lavage. As reported, we found irregular estrous cycles in all VIP KO females. Similarly, most of HT females presented irregular cycles compared to WT females (representative example shown in Fig. 1A). As expected, WT females had every proestrus immediately followed by estrus, whereas in VIP KO females this observation was significantly reduced (Fig. 1B). In addition, as depicted in Fig. 1C, VIP KO females exhibited prolonged periods in diestrus/metestrus, considered by the presence of leukocytes in smears, compared with WT females. VIP HT females showed an intermediate phenotype in every parameter measured.

Taking together these data suggest that VIP expression levels condition the regularity of the estrous cycle and fertility in females (Table 2).

3.2. Ovulation is impaired in young VIP-deficient females

Next, we assessed estradiol (E2) and progesterone (P4) production systemically (in serum) or locally (in ovary) in 3-months-old VIP KO, HT and WT females. We did not find statistical differences in the levels of E2 nor P4 systemically or locally (Table 1). However, we found that the ovaries were significantly lighter in HT and KO mice in comparison with WT from the same age. In order to elucidate causes of this difference in ovary weights, we quantified the number of follicles in ovarian slices stained with hematoxylin-eosin for each mouse group through all the stages of development (Fig. 2A–F). A significant reduction in the number of mature antral follicles and corpora lutea in comparison with WT ovaries was observed in ovaries from VIP KO females (Fig. 2D and E). On the other hand, VIP KO females also displayed a higher number of atretic follicles (Fig. 2F). These results reflect a dysfunctional ovary with follicles that do not finish maturation and undergo atresia.

We next evaluated the ovulation process *in vivo*. After 24 h of the appearance of the vaginal plug, VIP KO females were sacrificed and the number of oocytes and embryos found in the ovarian tubes were quantified. In 50 % of the VIP KO females, only oocytes were found indicating that there was no fertilization. In addition, 25 % of the KO females presented embryos that developed in culture without differences compared to those obtained from WT; and in the remaining 25 % neither embryos nor oocytes were found in the tubes indicating an ovulation failure (Fig. 2G). In contrast, embryos of 2 cells were found in 100 % of WT females as expected, with a normal evolution until the blastocyst stage in culture (Fig. 2G, the right panel shows a representative assay of a WT embryo development at different stages). Taken together, the present data suggest that VIP is necessary for ovulation.

Table 1
Primers used in RT-PCR assays. Oligonucleotide primers were designed using the online tool Primer3® (Whitehead Institute for Biomedical Research).

Primer	Sense	Sequence (5′ → 3′)	T
GapDH	F	TGATGACATCAAGAAGGTGGTGAAG	61°
	R	TCCTTGGAGGCCATGTAGGCCAT	
FOXP3	F	GGCCCTTCTCCAGGACAGA	61°
	R	GCTGATCATGGCTGGGTTGT	
RoRγt	F	CACGGCCCTGGTTCTCAT	58°
	R	CAGATGTTCCACTCTCCTCTTCTCT	
TGFβ	F	GACTCTCCACCTGCAAGACCA	60°
	R	TTGGGGGACTGGCGAGCCTT	
IL6	F	ACCGCTATGAAGTTCCTCTCTGC	58°
	R	AGTGGTATCCTCTGTGAAGTCTCC	

3.3. VIP deficient mice display premature aging characterized by an inflammatory ovarian microenvironment and the presence of foamy macrophages

Considering the properties of VIP as an anti-inflammatory mediator, we analyzed the ovarian immune microenvironment in VIP KO females. As shown in Fig. 3A, hematoxylin-eosin staining of ovarian tissue from young VIP KO females (3 months of age) shows a unique macrophage population with characteristics of “foamy macrophages” that was not found in WT females of the same age. These cells are evidenced as a partial replacement of the stromal component by clearer areas that are composed by multinucleated giant cells with a foamy cytoplasm and are representative of premature aging in mice models and humans [6,38–40]. The foamy areas were determined counting total cells *versus* foamy cells in 10 HPF- high power field- and were expressed as a relative percentage. As shown in Fig. 3B these areas appeared significantly increased in VIP KO ovaries, while HT ovaries presented only a slight increase. Next, IL-1ß secretion by the ovaries was tested as a classical inflammatory cytokine also associated to ovarian aging. IL-1ß secretion by young ovaries from VIP KO mice was increased in comparison with that secreted from WT female ovaries (see Fig. 3C).

The present results suggest that the absence of VIP induces a pro-inflammatory microenvironment that characterizes ovarian aging.

3.4. Premature aging associates with lighter ovaries and a dysregulation in hormonal production in VIP deficient mice

Considering that during normal aging ovarian weight decreases while body weight increases [41,42], we next evaluated the body and ovarian weight in 3 and 8 month old VIP KO, HT and WT mice. Surprisingly, ovarian weight was significantly reduced in young (3 months) VIP KO and HT females in comparison with WT, and this reduction was sustained also in older females (8 months) (see Fig. 4A). To ensure that the difference observed above was not related to a difference in body weight, we analyzed the body weight of young and aged females from the 3 groups. When comparing young females, no significant differences were observed in body weight between the different genotypes (Fig. 4B), therefore, the difference obtained in the ovarian weight is not due to differences in body weight. In fact, VIP KO females did not increase body weight with age as did the females from the WT and HT group (Fig. 4B).

Since the increase in the body weight is associated with a fall in E2 levels in serum, we next quantified E2 and P4 levels in young and old females (3 and 8 months old). As depicted in Fig. 4C, VIP KO mice showed higher levels of E2 in serum compared with their counterpart WT of 8 months. No differences were observed for P4 (Fig. 4D).

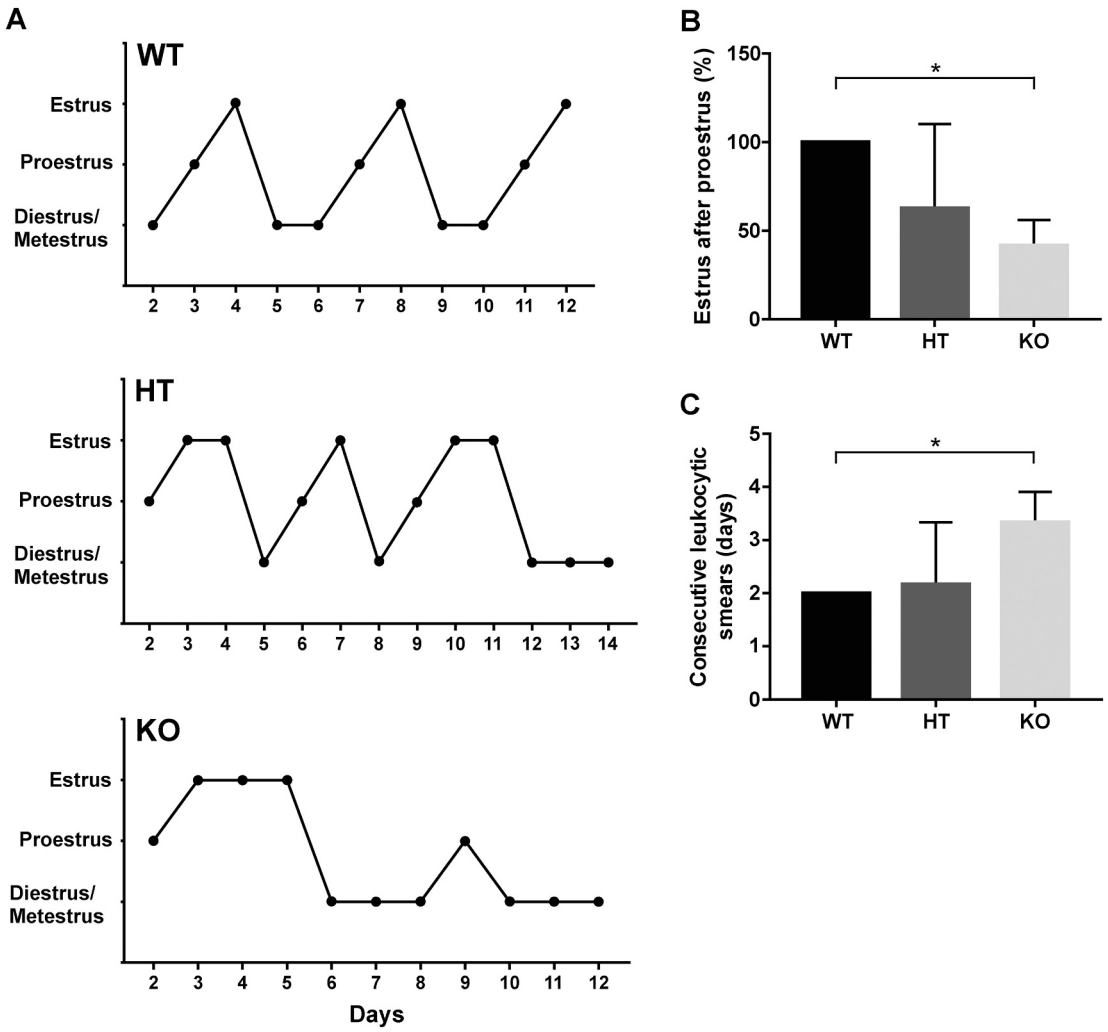

Fig. 1. Regularity of the estrous cycle is impaired in young VIP-deficient females. WT ($n = 5$), VIP HT (n = 5), and VIP KO (n = 5) female mice (3 months old) were monitored to determine the estrous cycle using vaginal lavage at the same time of the day (at Zeitgeber time (ZT)1) for 14 consecutive days. (A) Representative example of the regularity of the estrous cycle was determined. (B) Percentage of proestrus smears followed by estrus ± SEM. (C) Number of consecutive days in diestrus and metestrus in VIP KO, HT and WT females (Kruskal Wallis Test with Dunn's multiple comparison test $^*p < 0.05$).

Table 2
Ovarian and serum determinations of Estradiol and Progesterone in young VIP deficient females. Ovaries from WT ($n = 5$), VIP HT (n = 5), and VIP KO (n = 5) female mice (3 months old) were extracted, weighed, and used for Estradiol and Progesterone determinations by RIA. Results are expressed as mean of ng/mg protein ± SEM. In parallel, serum from the same animals was used to quantify estradiol and progesterone systemically. Results are expressed as mean of ng/ml for progesterone or pg/ml for Estradiol ± SEM. (Kruskal Wallis Test with Dunn's multiple comparison test).

Groups	Ovaries	Ovarian weight (mg) ± SEM	Estradiol ± SEM		Progesterone ± SEM	
			Serum (pg/ml)	Ovary (ng/mg prot.)	Serum (pg/ml)	Ovary (ng/mg prot.)
WT	5	5.583 ± 0.660	49.38 ± 8.10	1.047 ± 0.066	4.473 ± 0.90	4.227 ± 1.060
HT	5	4.022 ± 0.276*	40.43 ± 7.63	1.826 ± 0.314	2.390 ± 0.15	5.063 ± 0.763
KO	5	3.457 ± 0.266*	59.23 ± 18.60	0.780 ± 0.030	6.110 ± 2.17	7.116 ± 1.133

* $p < 0.05$.

The present results suggest, on one hand, that the differences found in ovarian weight may be due to the reduced number of corpora lutea in VIP KO females which are the main contributors to ovarian final weight. On the other hand, VIP KO females did not gain body weight by the advanced age and this could be explained by the sustained production of E2.

The adoptive transfer (AT) of regulatory T cells to VIP KO females is recruited toward the ovary and improved pregnancy rate.

In order to ameliorate the inflammation that we had previously noticed in VIP KO and HT uterus [23] and now also in the ovaries, we performed an adoptive transfer (AT) of Tregs (FOXP3+) to VIP KO females. Tregs were sorted FOXP3-GFP+ cells from inguinal and mesenteric lymph nodes from FOXP3 + GFP+ knock-in females and were transferred to 3-months infertile VIP KO females. After 48 h females were sacrificed and CD4 + FOXP3+ cells were quantified in ovaries, uterus, para-aortic lymph nodes (PLN) and spleen. As depicted in Fig. 5A, we observed a selective recruitment of Tregs to the ovary in relation to CD4+ cells in comparison with other tissues analyzed, as uterus and para-aortic lymph nodes (PLN) (and spleen, data not shown). The same results were observed when we analyzed Tregs relative to the number of cells injected (Fig. 5B). Fig. 5C shows representative dotplots from ovary, uterus and para-aortic lymph node.

In another set of experiments, those females that received the

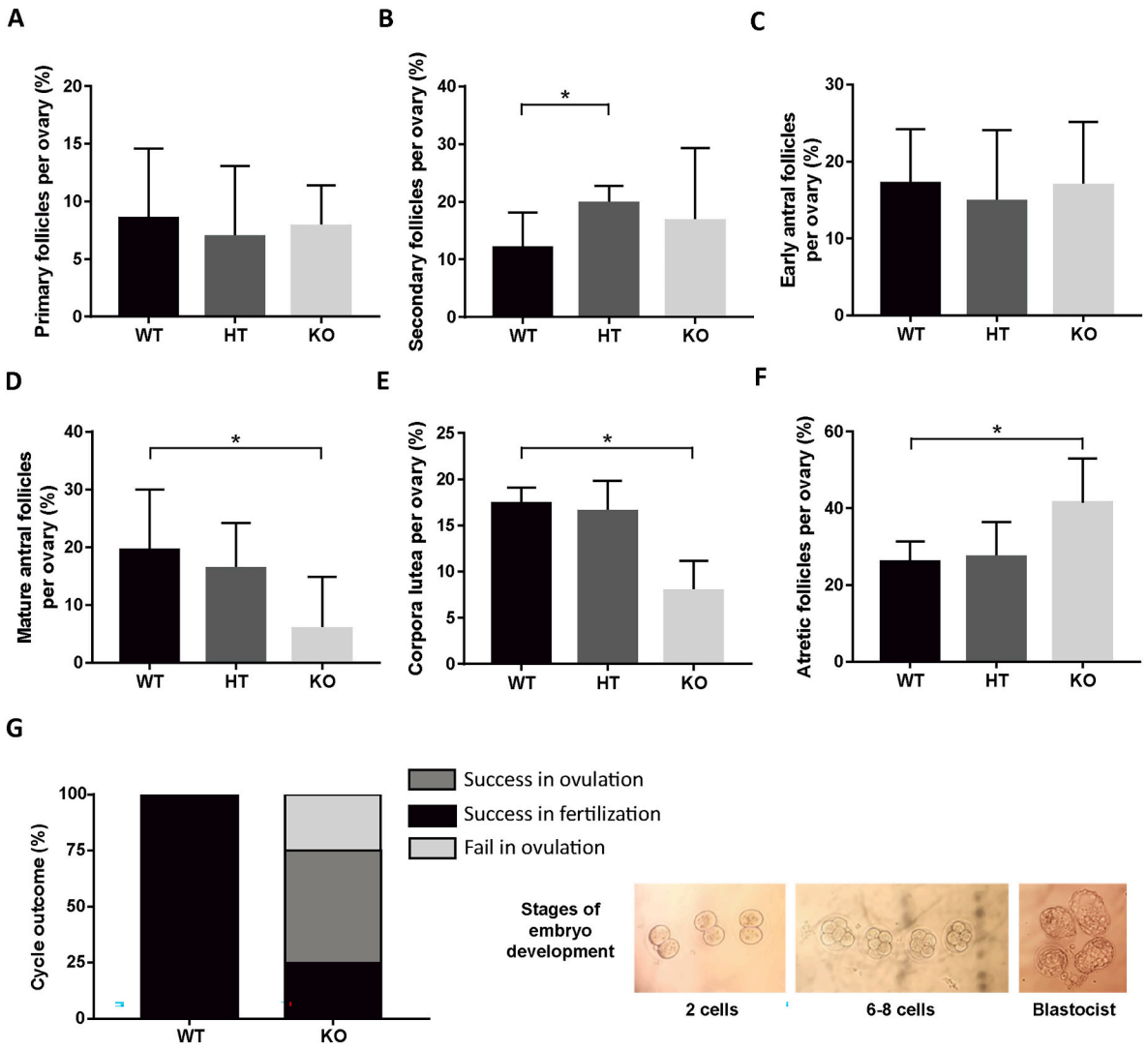

Fig. 2. Ovaries are dysfunctional in young VIP-deficient females. Ovaries from WT ($n = 5$), VIP HT (n = 5), and VIP KO (n = 5) female mice (3 months old) were obtained at Zeitgeber time (ZT)1 and used to perform histological quantifications of the number of follicles through all the development stages in histological ovarian slides stained with hematoxylin-eosin. Number of (A) primordial follicles, (B) secondary follicles, (C) early antral follicles, (D) mature antral follicles, (E) corpora lutea and (F) atretic follicles. Data are expressed as the mean ± SEM. Statistical analyses were performed by one-way ANOVA followed by Tukey's multiple-comparison test (*$p < 0.05$). (G) Effect of VIP deficiency in the cycle outcome in VIP KO in comparison with WT females. The right panel shows a representative example of a normal development from 2 cells to blastocyst stage *in vitro* of a WT sample.

adoptive transfer were mated with WT males, particularly with the same males that could not get the females pregnant previously. After vaginal plugs were observed, females were sacrificed at d5.5 of gestation and Tregs were quantified in several tissues. As displayed in Fig. 6A and B, we also observed an increase of Tregs recruitment toward the ovary in comparison with para-aortic lymph node (and spleen, data not shown). However, both ovaries and implantation sites displayed an enrichment of Tregs inside the CD4+ population that could be explained by the fact that both tissues represent immune-privilege sites (Fig. 6A and B). Fig. 6C shows representative dotplots from ovary, implantation sites and para-aortic lymph node.

An interesting point as that 66 % of the animals injected could finally get pregnant whereas the pregnancy rate in VIP KO females that did not receive the Tregs transfer was 26 % [23].

These results suggest that the Tregs transferred were selectively recruited toward the ovary and might improve the immune microenvironment to reach a successful pregnancy; when pregnancy is achieved, Tregs are recruited to both immune-privilege sites.

3.5. Adoptive transfer (AT) of FOXP3+ cells improves ovarian microenvironment

Considering that after adoptive transfer in VIP KO females improved pregnancy rate [23] and could modulate the immune microenvironment, we analyzed the expression of transcription factors and pro/anti-inflammatory mediators associated with a homeostatic microenvironment.

Treg FOXP3+ population display suppressive action on effector T cells and macrophages through the production of TGFβ and a local tolerogenic microenvironment which is also accompanied by a decrease in RORγt expression (transcription factor associated with a Th17 profile) and in IL-6 (a classical inflammatory cytokine associate with the induction of Th17 profile). On this basis we next evaluated the expression of FOXP3, RORγt, TGFβ and IL-6 by RT-PCR. As depicted in Fig. 7A–C, after adoptive transfer, a significant increase in FOXP3 expression was observed, while RORγt expression was not modulated implying an increase in Treg/Th17 ratio. Moreover, even though TGFβ expression was not modulated, a significant reduction in IL-6 expression was observed

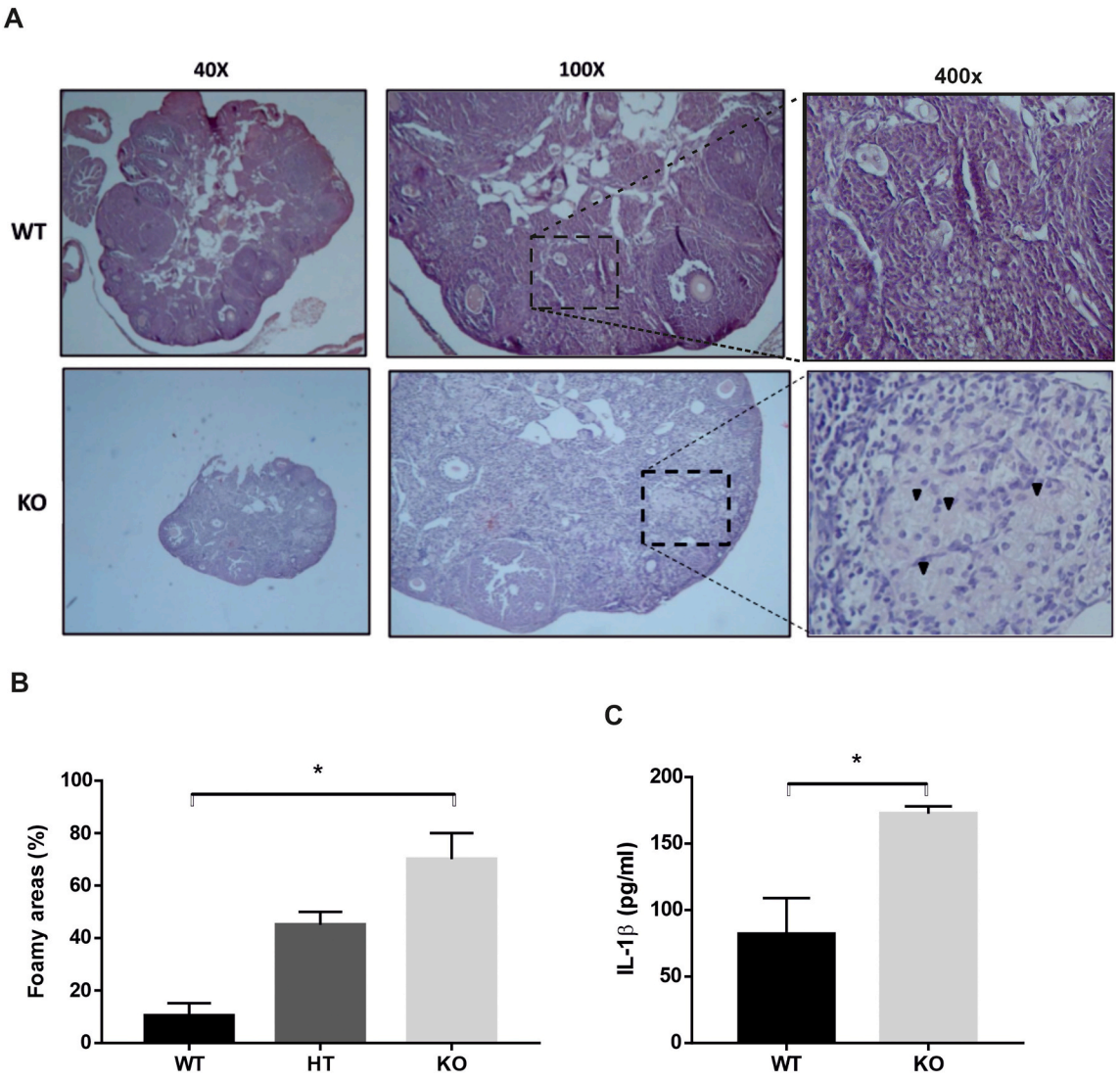

Fig. 3. VIP deficient mice display premature ovarian aging characterized by inflammation and the presence of foamy macrophages. Ovaries from WT ($n = 5$), VIP HT (n = 5), and VIP KO (n = 5) female mice (3 months old) were extracted at Zeitgeber time (ZT)1, fixed and embedded in paraffin wax to perform histological determinations. (A) Representative hematoxylin-eosin stained of ovarian tissue from young VIP KO and WT individuals. Figures from VIP KO females show partial replacement of stromal component by clearer areas (100×), that are composed by multinucleated big cells, with a foamy cytoplasm indicated with black arrows (400×) (B) Foamy areas measured in KO, HT and WT mice. The quantification of foamy cells was done counting total cells *versus* foamy cells in 10 HPF- high power field- and was expressed as a relative percentage (Kruskal Wallis Test with Dunn's multiple comparison test $*p < 0.05$) (C) IL-1ß secretion by young ovaries from VIP KO and WT females in culture for 48 h measured by ELISA. Results are expressed as mean pg/ml ± SEM (Mann Whitney test, $*p < 0.05$).

and, therefore, an increased TGFβ/IL-6 ratio (Fig. 7D–E).

The overall picture indicates that the adoptive transfer of FOXP3+ cells induces a local tolerogenic response improving ovarian microenvironment in favor of decreasing inflammation.

4. Discussion

Pregnancy success relies on multiple synchronized processes and interconnection of the immune, endocrine and reproductive systems. Understanding the ovarian microenvironment changes during reproductive aging could give new clues and insight on how gamete quality declines.

Here we demonstrated the relevance of maternal VIP to ovarian physiology and its implication in premature aging. First, VIP KO females presented completely irregular cycles. Second, dysfunctional ovaries with an increase in the number of atretic follicles and a decrease in the number of corpora lutea were found, generating ovaries with a lower ovulation rate. Third, we found a pro-inflammatory milieu with increased levels of IL-1β and the presence of a unique macrophage subpopulation identified as "foamy macrophages" that is associated with exacerbated inflammation. Finally, the subfertility noticed in VIP KO females was partially reversed by the adoptive transfer of Tregs (FOXP3+). The follow up of these cells showed that Tregs were selectively recruited to the ovary. In fact, it increased FOXP3/RORγt and TGFβ/IL-6 ratios improving ovarian immune microenvironment and pregnancy rate.

The overall picture reflects that VIP deficiency would generate not only a dysregulation in E2 secretion, leading to irregular estrous cycles, but also contribute to the generation of an inflammatory microenvironment impacting in ovarian physiology. In this sense, VIP displays multiple roles in the regulation of steroidogenic enzymes such as the regulatory protein (StAR) [43], the cytochrome P450 cholesterol side-chain cleavage enzyme complex (P450scc) and 17a-hidroxilase (17a-OH) [44] and aromatases [45], impacting on estrous cycles. Hence, dysregulation in E2 might increase atresia, which would generate a large number of apoptotic bodies that could generate foamy macrophages and

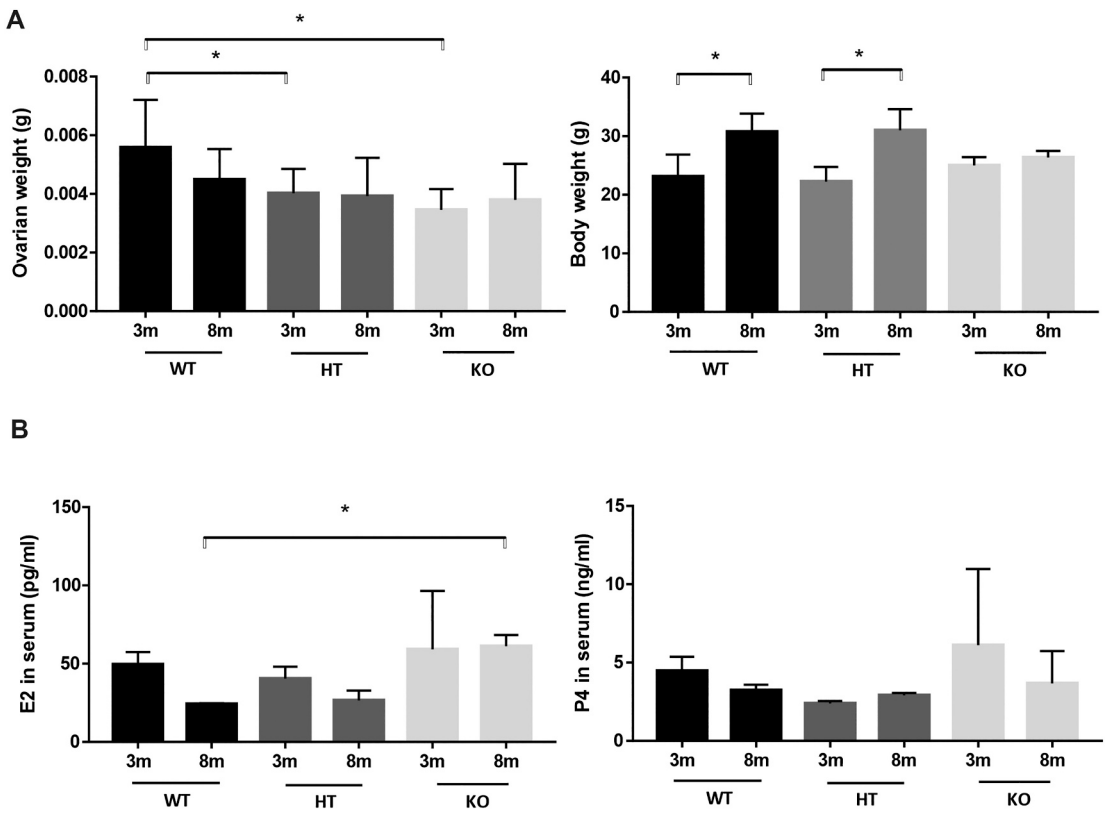

Fig. 4. VIP deficient mice displayed premature aging associated with lighter ovaries and a dysregulated hormonal production. Female from 3 or 8-month-old WT (n = 5), HT (n = 5) and VIP KO (n = 5) at Zeitgeber time (ZT)1 on the day of an estrus smear were sacrificed. (A) Ovarian and body weight was determined. (B) E2 and P4 production in serum was quantified by RIA. Values represent mean ± SEM of at least 5 animals (2way ANOVA with Tukey's multiple comparison test *$p < 0.05$).

a pro-inflammatory microenvironment. However, the mechanism of foamy macrophages differentiation should be further investigated.

VIP might participate in the regulation of the hypothalamic-pituitary-ovarian axis at multiple levels. At the SCN, VIP is released directly in the middle preoptic area of GnRH neurons [46,47]. GnRH neurons display a cyclic pattern that regulates the luteinizing hormone (LH) surge necessary for ovulation. Since VIP displays effects on GnRH neurons, it may provide an excitatory signal from the circadian clock that helps GnRH surge [48]. At the ovarian level VIP not only regulates the steroidogenesis but also survival and growth of the ovarian follicle and oocyte maturation [13,49].

When we compared WT and VIP KO females in advanced age we did not observe the expected fall in E2, neither the weight gain associated with aging [41,42]. Furthermore, comparing aged animals we found that VIP KO females presented very high E2 values in serum compared to WT females of the same age. Reproductive aging is characterized by delayed and attenuated levels of LH surge in response to E2 due to a decrease in the activity of GnRH neurons. Several hypothalamic neuropeptides including VIP drive the E2-mediated increase in GnRH/LH and appear to dampen with age or to lack the precise time coordination required for a specific GnRH secretion pattern [48]. In line with these reports, mature follicles of VIP KO mice did not become ovulated and die whereas there was an increased number of atretic follicles, strongly suggesting that lower LH peak levels associated with VIP deficiency entail ovulation failures. In support of this conclusion, we demonstrated that in 25 % of VIP KO females the oocytes were not ovulated.

Data from previous reports on VIP within the ovary focused on the regulation of the steroidogenic activity and its role in disrupted estrous cycle [16,30]. However, the immunomodulatory effects of VIP in the ovary have not been explored yet. Nevertheless, we do know the relevance of endogenous VIP to achieve a successful pregnancy as VIP KO mice exhibit some features of adverse pregnancy outcome and defective immune tolerance [20].

Regarding the reduction in the number of corpora lutea (CL) in the KO, in parallel with maintained P4 levels, we might consider that CL may reflect ovulation failure with more follicles that can't complete their maturation process and lead to atresia. Moreover, the maintained levels of P4 could be explained by a difference in the amount of periovulatory follicles that weren't analyzed in this study but represent also a P4 source within the ovary. It is worth to mention that LH modify the steroid enzymatic pathway transforming an estrogen secreting structure, the preovulatory follicle, into a P4-producing one (periovulatory follicle) by inducing a process of follicle luteinization before ovulation and CL formation [50,51]. In fact, the reduced percentage of CL without change in P4 levels in the ovaries could be also explain by the modulation of the crucial enzymes regulate the main steps of steroidogenesis. Particularly, it could be due to a possible slight increase in the expression of 3β-HSD and/or a reduction in the expression of CYP17 in luteal cells to compensate for the low number of CL. In line with this explanation, the observed increase in E2 levels could be due to an increase in the levels of the enzyme P450aromatase (CYP19) in granulosa cells. Further research in the expression of theses enzymes and its effect on steroidogenesis in ovaries from KO mice should be examined more closely.

Results presented here clearly show an inflammatory microenvironment in the ovaries from VIP KO females associated with the presence of foamy macrophages and with the increased production of IL-1β. The clearance of apoptotic bodies and chronic accumulation of phospholipids from these bodies lead to the accumulation of lipid droplets that remain intracellularly as indigestible substances [52]. Here, we found an increase in atresia, which would generate an increase in apoptotic bodies that need to be efficiently removed by phagocytosis to restore tissue homeostasis. This impaired efferocytosis in a proinflammatory context for long periods could generate foamy macrophages. Moreover, the foamy macrophages secrete pro-inflammatory

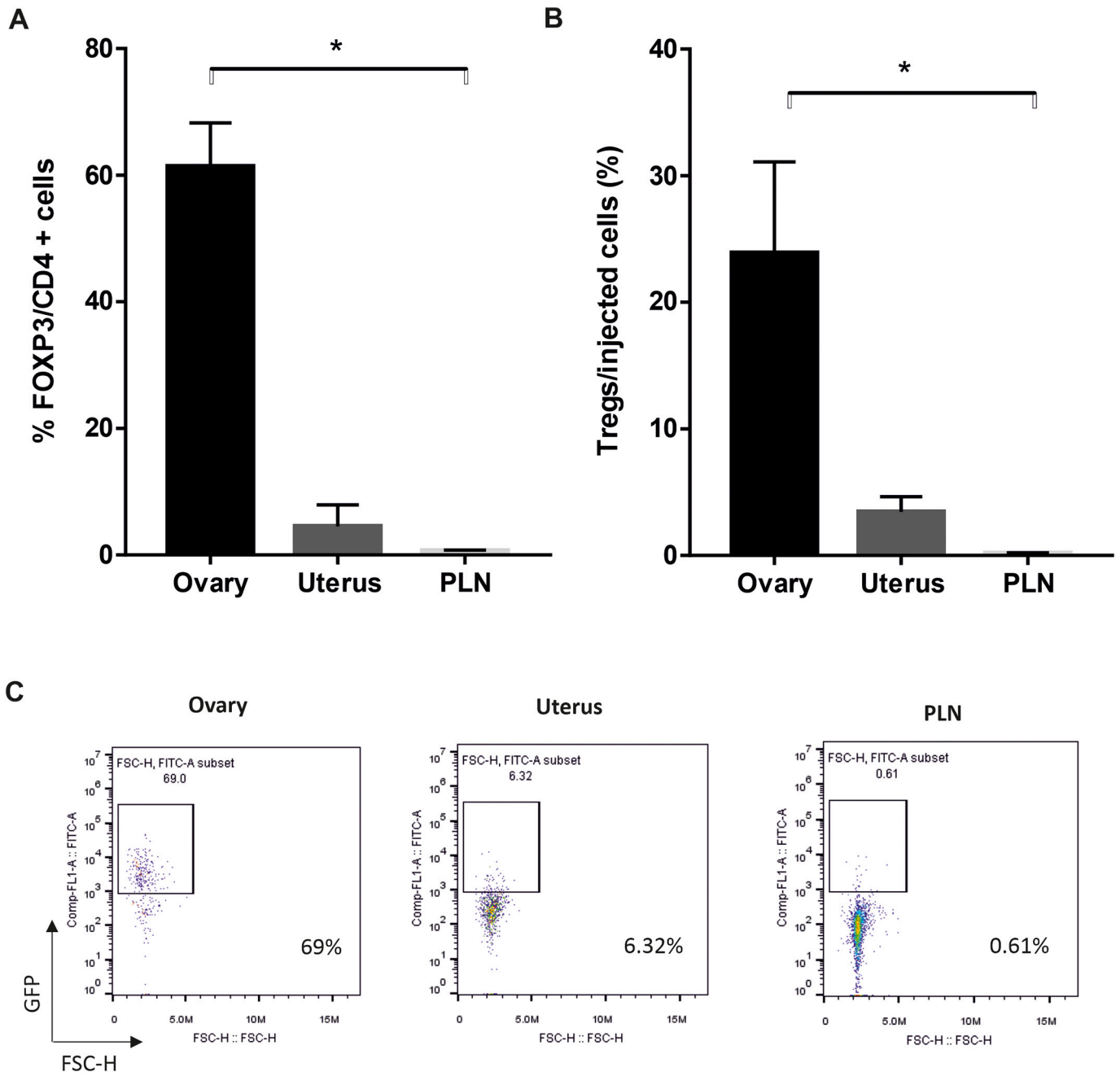

Fig. 5. Adoptive transfer (AT) of regulatory T cells to VIP KO non-pregnant mice. Tregs, FOXP3-GFP cells obtained from FOXP3-GFP-knock-in female were transferred to VIP KO infertile females 3 months old ($n = 4$). After 48 h, females were sacrificed at Zeitgeber time (ZT)1, tissues recovered and (A) CD4 + FOXP3+ cells frequency in ovaries, uterus and para-aortic lymph nodes (PLN) analyzed. Results are expressed as mean % CD4 FOXP3+ cells ± SEM of at least three females. (B) FOXP3 + GFP+ frequency in ovaries, uterus and PLN from the 200,000 Treg cells injected. (C) Figure shows representative dot plots of the frequency of FOXP3+ cells (inside the electronically gated CD4+) after AT, in ovary, uterus and PLN. Negative control samples were incubated in parallel with an irrelevant, isotype-matched Ab and used for cut-off setting (Kruskal Wallis Test with Dunn's multiple comparison test $^*p < 0.05$).

cytokines as IL-1β, IL-6 and TNFα generating a positive feedback loop of the inflammatory response leading to its chronicity [52].

In this sense, the IL-1β production is physiologically needed in the mammalian ovary during ovulation, menstruation, and implantation [53,54]. However, higher concentrations are associated with inflammatory conditions and may affect ovarian reserve [55,56]. Using IL-1α–KO and IL-1β–KO models, it was demonstrated the role of IL-1 in targeting genes associated with female reproductive aging and a mutual regulation of both IL-1 members [39,57,58].

Ovaries from middle aged mice were found to be more rigid compared to those from reproductively young mice, suggesting the presence of age-associated fibrosis and inflammation [59]. In fact, Duncan et al., using complementary approaches as histological, biochemical and cellular techniques, found a clear association of inflammatory mediators with the presence of multinucleated macrophage giant cells. Also, it was reported that the increase of multinucleated giant cells that arise from macrophages undergo fusion with other macrophages in an inflammatory context [60,61].

On the other hand, low number and/or reduced immunosuppressive function of Tregs in the decidua at the peri-implantation period would fail to achieve resolution of the inflammation as reported in murine models and in women with recurrent pregnancy loss [23,62,63]. Tregs

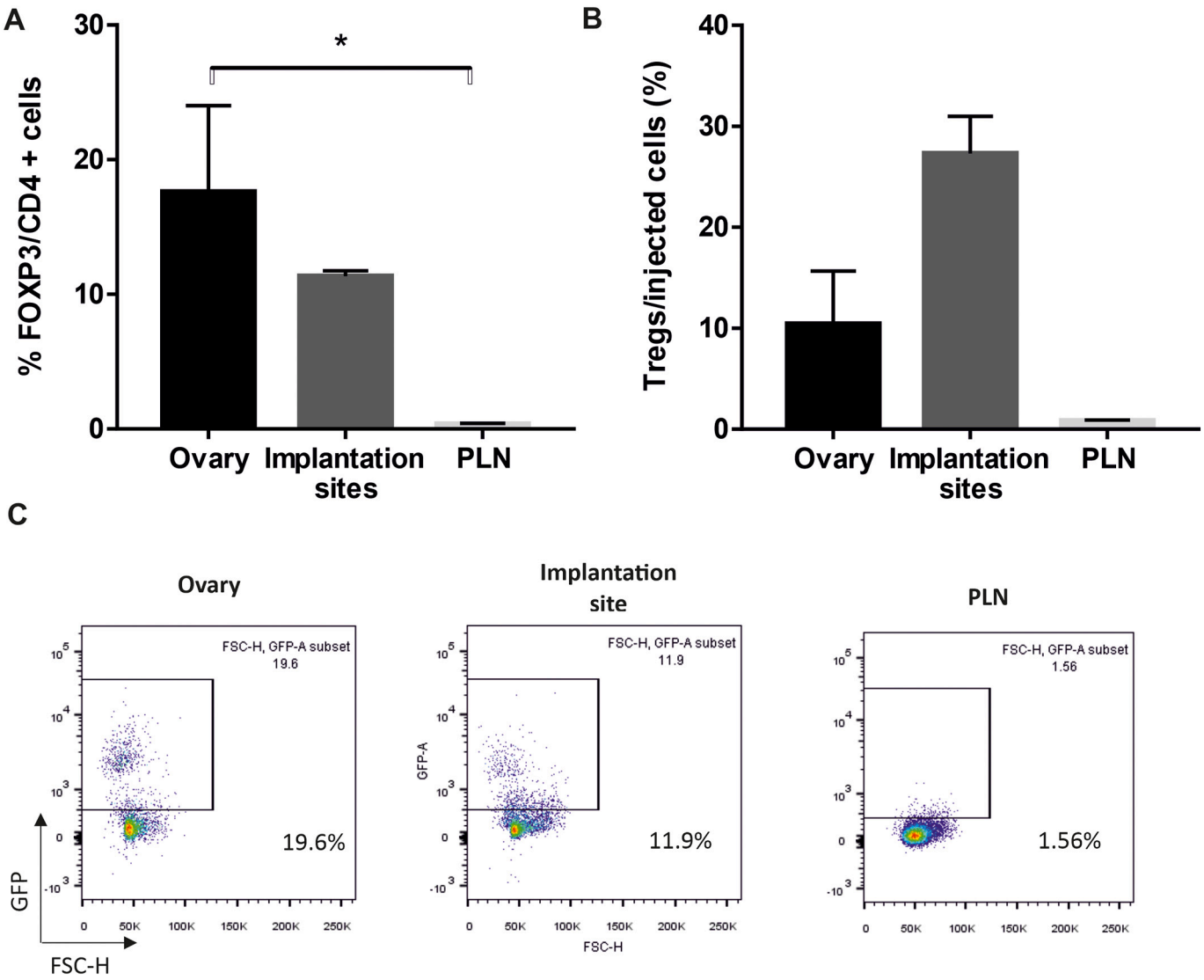

Fig. 6. Adoptive transfer (AT) of regulatory T cells to VIP KO pregnant mice. Tregs, FOXP3-GFP cells obtained from FOXP3-GFP-knock-in female were transferred to VIP KO infertile females 3 months old ($n = 4$). After the adoptive transfer (AT), the injected females were mated. Five days after the visualization of the vaginal plug, they were sacrificed and the ovaries, implantation sites and para-aortic lymph nodes (PLN) obtained at Zeitgeber time (ZT)1. (A) CD4 + FOXP3+ cells frequency in ovaries, implantation sites and para-aortic lymph nodes (PLN). Results are expressed as mean % CD4 FOXP3+ cells ± SEM of at least three females. (B) FOXP3 + GFP+ frequency in ovaries, implantation sites and PLN from the 200,000 Treg cells injected. (C) Figure shows representative dot plots of the frequency of FOXP3+ cells (inside the electronically gated CD4+) after AT, in ovary, implantation sites and PLN. Negative control samples were incubated in parallel with an irrelevant, isotype-matched Ab and used for cut-off setting. (Kruskal Wallis Test with Dunn's multiple comparison test $^*p < 0.05$).

injected in VIP KO females that could not get pregnant were mainly recruited to the ovary. Moreover, we reported a significant increase in the pregnancy rate of subfertile females, indicating that these cells must reduce inflammation and therefore improve their fertility. Supporting these findings, here we found an increased FOXP3/RORγt and TGFβ/IL-6 ratio. FOXP3 adoptive transfer not only improved ovarian microenvironment favoring an anti-inflammatory response, it also increased pregnancy rate. This finding is in accordance with what was found recently using a POI (primary ovarian insufficiency) model where the adoptive transfer of Tregs was able to improve many aspects of this ovarian autoimmune disorder [65]. In another mouse model presenting chemotherapy-induced primary ovarian failure, the increase in Tregs reduced the inflammatory reaction and contributed to restore ovarian function [66].

In conclusion, evidence presented here supports that VIP deficiency allows a premature reproductive aging and infertility through the generation of an inflammatory milieu in the ovary accompanied by hormonal dysregulation. Therefore, VIP might be a potential and promising biomarker for improving reproductive function in the context of age-related infertility and fertility preservation.

Considering that mice at 7–9 months of age correspond to 38–45 years on a linear extrapolation to women age [6], and the current social context that leads women to postpone motherhood to this age [64], the present *in vivo* model represents a useful approach to the mechanisms of reproductive inflammaging.

CRediT authorship contribution statement

CPL and RR designed the study, supervised the experimental work and wrote the manuscript together with JW. LG, VH, DV and LC carried out all the experiments, data analysis and interpretation using the VIP KO, HT and WT mice. ZN performed daily mice examination. FP and NP performed all the follicles analysis. LG and FM performed Tregs assays. MM performed the histology analysis and VF fecundation tests. CPL and

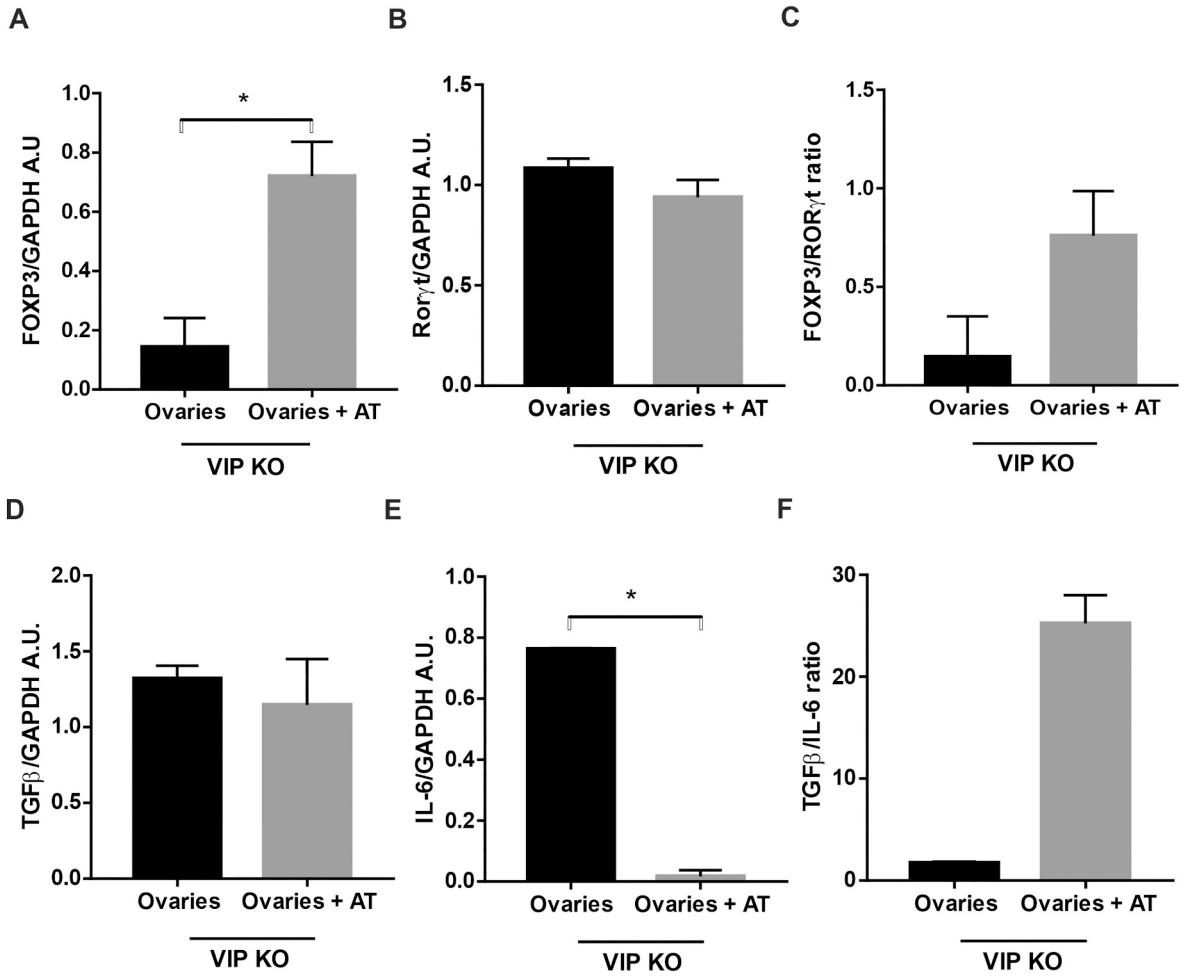

Fig. 7. Adoptive transfer (AT) of FOXP3+ cells improves ovarian immune microenvironment. Tregs, FOXP3-GFP+ cells obtained from FOXP3-GFP-knock-in female were transferred to VIP KO infertile females 3 months old (n = 4). After 48 h females were sacrificed, ovaries recovered and analyzed. Expression of transcription factors and mediators were evaluated by RT-PCR in ovaries pre and post adoptive transfer (AT). (A) FOXP3, (B) RORγt expression and (C) FOXP3/RORγt ratio. (D) TGFβ, (E) IL-6 expression and (F) TGFβ/IL-6 ratio. Bands were semi-quantified with ImageJ® and intensity expressed in arbitrary units (A.U.) relative to GAPDH. Values represent mean ± SEM of at least 3 experiments (Mann Whitney test $*p < 0.05$).

RR supervised the whole study. All authors read and approved the final manuscript.

Declaration of competing interest

The authors declare that they have no known competing financial interests or personal relationships that could have appeared to influence the work reported in this paper.

Data availability

The data that support the findings of this study are available from the corresponding author upon reasonable request.

Acknowledgements

This work was funded by the National Agency of Sciences and Technology ANPCyT (PICT 2018-4715 and 2018-2461 to RR, 2019-1554 to CPL), and University of Buenos Aires (UBACyT 20020170100317BA to CPL and UBACyT 20020090200034 to RR).

References

[1] F.J. Broekmans, M.R. Soules, B.C. Fauser, Ovarian aging: mechanisms and clinical consequences, Endocr. Rev. 30 (5) (2009) 465–493, https://doi.org/10.1210/er.2009-0006.
[2] S.I. Nagaoka, T.J. Hassold, P.A. Hunt, Human aneuploidy: mechanisms and new insights into an age-old problem, Nat. Rev. Genet. 13 (7) (2012) 493–504, https://doi.org/10.1038/nrg3245.
[3] A. Jagger, Y. Shimojima, J.J. Goronzy, C.M. Weyand, Regulatory T cells and the immune aging process: a mini-review, Gerontology 60 (2) (2014) 130–137, https://doi.org/10.1159/000355303.
[4] M.-A. Lim, J. Lee, J.-S. Park, J.-Y. Jhun, Y.-M. Moon, M.-L. Cho, H.-Y. Kim, Increased Th17 differentiation in aged mice is significantly associated with high IL-1β level and low IL-2 expression, Exp. Gerontol. 49 (2014) 55–62, https://doi.org/10.1016/j.exger.2013.10.006.
[5] V. Schmitt, L. Rink, P. Uciechowski, The Th17/Treg balance is disturbed during aging, Exp. Gerontol. 48 (12) (2013) 1379–1386, https://doi.org/10.1016/j.exger.2013.09.003.
[6] S.M. Briley, S. Jasti, J.M. Mccracken, J.E. Hornick, M.T. Pritchard, F.E. Duncan, Reproductive age-associated fibrosis in the stroma of the mammalian ovary 152 (3) (2017) 245–260, https://doi.org/10.1530/REP-16-0129.Reproductive.
[7] D.A. Clark, The importance of being a regulatory T cell in pregnancy, J. Reprod. Immunol. 116 (2016) 60–69, https://doi.org/10.1016/j.jri.2016.04.288.
[8] R.J. Heitmann, R.P. Weitzel, Y. Feng, J.H. Segars, J.F. Tisdale, E.F. Wolff, Maternal T regulatory cell depletion impairs embryo implantation which can be corrected with adoptive T regulatory cell transfer, Reprod. Sci. 24 (7) (2017) 1014–1024, https://doi.org/10.1177/1933719116675054.
[9] A. Schumacher, D.J. Sharkey, S.A. Robertson, A.C. Zenclussen, Immune cells at the fetomaternal Interface: how the microenvironment modulates immune cells to Foster fetal development, J. Immunol. 201 (2) (2018) 325–334, https://doi.org/10.4049/jimmunol.1800058.

[10] T. Shima, K. Inada, A. Nakashima, A. Ushijima, M. Ito, O. Yoshino, S. Saito, Paternal antigen-specific proliferating regulatory T cells are increased in uterine-draining lymph nodes just before implantation and in pregnant uterus just after implantation by seminal plasma-priming in allogeneic mouse pregnancy, J. Reprod. Immunol. 108 (2015) 72–82, https://doi.org/10.1016/j.jri.2015.02.005.

[11] S.I. Said, V. Mutt, Polypeptide with broad biological activity: isolation from small intestine, Science 169 (3951) (1970) 1217–1218, https://doi.org/10.1126/science.169.3951.1217.

[12] L.I. Larsson, J. Fahrenkrug, O. Schaffalitzky De Muckadell, F. Sundler, R. Håkanson, J.R. Rehfeld, Localization of vasoactive intestinal polypeptide (VIP) to central and peripheral neurons, Proc. Natl. Acad. Sci. 73 (9) (1976) 3197–3200, https://doi.org/10.1073/pnas.73.9.3197.

[13] J.B. Bruno, M.H.T. Matos, R.N. Chaves, J.R. Figueiredo, Involvement of vasoactive intestinal peptide (VIP) on ovarian physiology, Anim. Reprod. 8 (3/4) (2011) 51–57.

[14] R. Ramhorst, G. Calo, D. Paparini, D. Vota, V. Hauk, L. Gallino, C.P. Leirós, Control of the inflammatory response during pregnancy: potential role of VIP as a regulatory peptide, Ann. N. Y. Acad. Sci. 1437 (1) (2019) 15–21, https://doi.org/10.1111/nyas.13632.

[15] J. Benjamin Davoren, A.J.W. Hsueh, Vasoactive intestinal peptide: a novel stimulator of steroidogenesis by cultured rat granulosa Cells1, Biol. Reprod. 33 (1) (1985) 37–52, https://doi.org/10.1095/biolreprod33.1.37.

[16] C. Parra, J.L. Fiedler, S.L. Luna, M. Greiner, V. Padmanabhan, H.E. Lara, Participation of vasoactive intestinal polypeptide in ovarian steroids production during the rat estrous cycle and in the development of estradiol valerate-induced polycystic ovary, Reproduction 133 (1) (2007) 147–154, https://doi.org/10.1530/rep.1.01214.

[17] W.H. Trzeciak, C.E. Ahmed, E.R. Simpson, S.R. Ojeda, Vasoactive intestinal peptide induces the synthesis of the cholesterol side-chain cleavage enzyme complex in cultured rat ovarian granulosa cells, Proc. Natl. Acad. Sci. 83 (19) (1986) 7490–7494, https://doi.org/10.1073/pnas.83.19.7490.

[18] E. Grasso, D. Paparini, M. Agüero, G. Mor, C. Pérez Leirós, R. Ramhorst, VIP contribution to the decidualization program: regulatory T cell recruitment, J. Endocrinol. 221 (1) (2014) 121–131, https://doi.org/10.1530/JOE-13-0565.

[19] E. Grasso, D. Paparini, V. Hauk, G. Salamone, C.P. Leiros, R. Ramhorst, Differential migration and activation profile of monocytes after trophoblast interaction, PloS One 9 (5) (2014), e97147, https://doi.org/10.1371/journal.pone.0097147.

[20] V. Hauk, D. Vota, L. Gallino, G. Calo, D. Paparini, F. Merech, C.P. Leirós, Trophoblast VIP deficiency entails immune homeostasis loss and adverse pregnancy outcome in mice, FASEB J. 33 (2) (2019) 1801–1810, https://doi.org/10.1096/fj.201800592RR.

[21] J. Waschek, VIP and PACAP: neuropeptide modulators of CNS inflammation, injury, and repair, Br. J. Pharmacol. 169 (3) (2013) 512–523, https://doi.org/10.1111/bph.12181.

[22] G. Calo, F. Sabbione, D. Vota, D. Paparini, R. Ramhorst, A. Trevani, C.P. Leirós, Trophoblast cells inhibit neutrophil extracellular trap formation and enhance apoptosis through vasoactive intestinal peptide-mediated pathways, Hum. Reprod. 32 (1) (2017), https://doi.org/10.1093/humrep/dew292.

[23] L. Gallino, V. Hauk, L. Fernández, E. Soczewski, S. Gori, E. Grasso, R. Ramhorst, VIP promotes recruitment of tregs to the uterine-placental Interface during the peri-implantation period to sustain a tolerogenic microenvironment, Front. Immunol. 10 (January) (2020), https://doi.org/10.3389/fimmu.2019.02907.

[24] V. Hauk, S. Azzam, G. Calo, L. Gallino, D. Paparini, A. Franchi, C.P. Leirós, Vasoactive intestinal peptide induces an immunosuppressant microenvironment in the maternal-fetal Interface of non-obese diabetic mice and improves early pregnancy outcome, Am. J. Reprod. Immunol. 71 (2) (2014) 120–130.

[25] R. Ramhorst, E. Grasso, D. Paparini, V. Hauk, L. Gallino, G. Calo, C. Pérez Leirós, Decoding the chemokine network that links leukocytes with decidual cells and the trophoblast during early implantation, Cell Adhesion & Migration 10 (1–2) (2016) 197–207, https://doi.org/10.1080/19336918.2015.1135285.

[26] G. Salamone, L. Fraccaroli, S. Gori, E. Grasso, D. Paparini, J. Geffner, R. Ramhorst, Trophoblast cells induce a tolerogenic profile in dendritic cells, Hum. Reprod. 27 (9) (2012) 2598–2606, https://doi.org/10.1093/humrep/des208.

[27] C. Abad, Y.V. Tan, Immunomodulatory roles of PACAP and VIP: lessons from knockout mice, J. Mol. Neurosci. 66 (1) (2018) 102–113, https://doi.org/10.1007/s12031-018-1150-y.

[28] C. Abad, Y.V. Tan, G. Cheung-Lau, H. Nobuta, J.A. Waschek, VIP deficient mice exhibit resistance to lipopolysaccharide induced endotoxemia with an intrinsic defect in proinflammatory cellular responses, PLoS ONE 7 (5) (2012), https://doi.org/10.1371/journal.pone.0036922.

[29] J.-M. Li, L. Southerland, M.S. Hossain, C.R. Giver, Y. Wang, K. Darlak, E.K. Waller, Absence of vasoactive intestinal peptide expression in hematopoietic cells enhances Th1 polarization and antiviral immunity in mice, Journal of Immunology (Baltimore, Md.: 1950) 187 (2) (2011) 1057–1065, https://doi.org/10.4049/jimmunol.1100686.

[30] D.H. Loh, D.A. Kuljis, L. Azuma, Y. Wu, D. Truong, H.B. Wang, C.S. Colwell, Disrupted reproduction, estrous cycle, and circadian rhythms in female mice deficient in vasoactive intestinal peptide, J. Biol. Rhythm. 29 (5) (2014) 355–369, https://doi.org/10.1177/0748730414549767.

[31] C.S. Colwell, S. Michel, J. Itri, W. Rodriguez, J. Tam, V. Lelievre, J.A. Waschek, Disrupted circadian rhythms in VIP- and PHI-deficient mice, Am. J. Phys. Regul. Integr. Comp. Phys. 285 (5) (2003) R939–R949, https://doi.org/10.1152/ajpregu.00200.2003.

[32] W. Lin, D. Haribhai, L.M. Relland, N. Truong, M.R. Carlson, C.B. Williams, T. A. Chatila, Regulatory T cell development in the absence of functional Foxp3, Nat. Immunol. 8 (4) (2007) 359–368, https://doi.org/10.1038/ni1445.

[33] C.S. Caligioni, Assessing reproductive Status/Stages in mice, Curr. Protoc. Neurosci. (2009), https://doi.org/10.1002/0471142301.nsa04is48.

[34] N. Pascuali, L. Scotti, D. Abramovich, G. Irusta, M. Di Pietro, D. Bas, F. Parborell, Inhibition of platelet-derived growth factor (PDGF) receptor affects follicular development and ovarian proliferation, apoptosis and angiogenesis in prepubertal eCG-treated rats, Mol. Cell. Endocrinol. 412 (2015) 148–158, https://doi.org/10.1016/j.mce.2015.04.021.

[35] N. Pascuali, L. Scotti, M. Di Pietro, G. Oubiña, D. Bas, M. May, F. Parborell, Ceramide-1-phosphate has protective properties against cyclophosphamide-induced ovarian damage in a mice model of premature ovarian failure, Hum. Reprod. 33 (5) (2018) 844–859, https://doi.org/10.1093/humrep/dey045.

[36] G. Irusta, F. Parborell, M. Tesone, Inhibition of cytochrome P -450 C17 enzyme by a GnRH agonist in ovarian follicles from gonadotropin-stimulated rats, Am. J. Physiol. Endocrinol. Metab. 292 (5) (2007) E1456–E1464, https://doi.org/10.1152/ajpendo.00226.2006.

[37] T. Woodruff, J. D'Agostino, N. Schwartz, K. Mayo, Dynamic changes in inhibin messenger RNAs in rat ovarian follicles during the reproductive cycle, Science 239 (4845) (1988) 1296–1299, https://doi.org/10.1126/science.3125611.

[38] I. Ben-Aharon, M. Levi, D. Margel, R. Yerushalmi, S. Rizel, S. Perry, S.M. Stemmer, Premature ovarian aging in BRCA carriers: a prototype of systemic precocious aging? Oncotarget 9 (22) (2018) 15931–15941, https://doi.org/10.18632/oncotarget.24638.

[39] S. Uri-Belapolsky, A. Shaish, E. Eliyahu, H. Grossman, M. Levi, D. Chuderland, Y. Kamari, Interleukin-1 deficiency prolongs ovarian lifespan in mice, Proceedings of the National Academy of Sciences of the United States of America 111 (34) (2014) 12492–12497, https://doi.org/10.1073/pnas.1323955111.

[40] Z. Yang, Z. Tang, X. Cao, Q. Xie, C. Hu, Z. Zhong, Y. Zheng, Controlling chronic low-grade inflammation to improve follicle development and survival, American Journal of Reproductive Immunology 84 (2) (2020) 0–3, https://doi.org/10.1111/aji.13265.

[41] M.K. Beard, L.R. Curtis, Libido, menopause, and estrogen replacement therapy, Postgrad. Med. 86 (1) (1989) 225–228, https://doi.org/10.1080/00325481.1989.11704338.

[42] J.F. Nelson, R.G. Gosden, L.S. Felicio, Effect of dietary restriction on estrous cyclicity and follicular reserves in aging C57BL/6J mice 1, Biol. Reprod. 32 (3) (1985) 515–522, https://doi.org/10.1095/biolreprod32.3.515.

[43] M.P. Kowalewski, M.T. Dyson, A. Boos, D.M. Stocco, Vasoactive intestinal peptide (VIP)-mediated expression and function of steroidogenic acute regulatory protein (StAR) in granulosa cells, Mol. Cell. Endocrinol. 328 (1–2) (2010) 93–103, https://doi.org/10.1016/j.mce.2010.07.018.

[44] A.L. Johnson, Z. Li, J.A. Gibney, S. Malamed, Vasoactive intestinal peptide-induced expression of cytochrome P450 cholesterol side-chain cleavage and 17α-hydroxylase enzyme activity in hen granulosa Cells1, Biol. Reprod. 51 (2) (1994) 327–333, https://doi.org/10.1095/biolreprod51.2.327.

[45] F.W. George, S.R. Ojeda, Vasoactive intestinal peptide enhances aromatase activity in the neonatal rat ovary before development of primary follicles or responsiveness to follicle-stimulating hormone, Proc. Natl. Acad. Sci. 84 (16) (1987) 5803–5807, https://doi.org/10.1073/pnas.84.16.5803.

[46] L.J. Kriegsfeld, R. Silver, A.C. Gore, D. Crews, Vasoactive intestinal polypeptide contacts on gonadotropin-releasing hormone neurones increase following puberty in female rats, J. Neuroendocrinol. 14 (9) (2002) 685–690, https://doi.org/10.1046/j.1365-2826.2002.00818.x.

[47] D.R. Ward, F.M. Dear, I.A. Ward, S.I. Anderson, D.J. Spergel, P.A. Smith, F.J. P. Ebling, Innervation of gonadotropin-releasing hormone neurons by peptidergic neurons conveying circadian or energy balance information in the mouse, PLoS ONE 4 (4) (2009), e5322, https://doi.org/10.1371/journal.pone.0005322.

[48] C.A. Christian, S.M. Moenter, Vasoactive intestinal polypeptide can excite gonadotropin-releasing hormone neurons in a manner dependent on estradiol and gated by time of day, Endocrinology 149 (6) (2008) 3130–3136, https://doi.org/10.1210/en.2007-1098.

[49] S. Streiter, B. Fisch, B. Sabbah, A. Ao, R. Abir, The importance of neuronal growth factors in the ovary, Mol. Hum. Reprod. 22 (1) (2015) 3–17, https://doi.org/10.1093/molehr/gav057.

[50] B. Berisha, M. Steffl, H. Welter, H. Kliem, H.H.D. Meyer, D. Schams, W. Amselgruber, Effect of the luteinising hormone surge on regulation of vascular endothelial growth factor and extracellular matrix-degrading proteinases and their inhibitors in bovine follicles, Reprod. Fertil. Dev. 20 (2) (2008) 258, https://doi.org/10.1071/RD07125.

[51] J.E. Fortune, E.L. Willis, P.J. Bridges, C.S. Yang, The periovulatory period in cattle: progesterone, prostaglandins, oxytocin and ADAMTS proteases, Retrieved from, Anim. Reprod. 6 (1) (2009) 60–71, http://www.ncbi.nlm.nih.gov/pubmed/20390049.

[52] H.Z. Ford, L. Zeboudj, G.S.D. Purvis, A. Ten Bokum, A.E. Zarebski, J.A. Bull, D. R. Greaves, Efferocytosis perpetuates substance accumulationinsidemacrophagepopulations, Proc. R. Soc. B Biol. Sci. 286 (1904) (2019), https://doi.org/10.1098/rspb.2019.0730.

[53] N. Gerard, M. Caillaud, A. Martoriati, G. Goudet, A. Lalmanach, The interleukin-1 system and female reproduction, J. Endocrinol. 180 (2) (2004) 203–212, https://doi.org/10.1677/joe.0.1800203.

[54] H.N. Jabbour, K.J. Sales, R.D. Catalano, J.E. Norman, Inflammatory pathways in female reproductive health and disease, Reproduction 138 (6) (2009) 903–919, https://doi.org/10.1530/REP-09-0247.

[55] H. Falconer, J. Sundqvist, K. Gemzell-Danielsson, B. von Schoultz, T. D'Hooghe, G. Fried, IVF outcome in women with endometriosis in relation to tumour necrosis factor and anti-Müllerian hormone, Reprod. BioMed. Online 18 (4) (2009) 582–588, https://doi.org/10.1016/S1472-6483(10)60138-1.
[56] T. Fréour, C. Miossec, K. Bach-Ngohou, T. Dejoie, M. Flamant, O. Maillard, D. Masson, Ovarian Reserve in Young Women of reproductive age with Crohn's disease, Inflamm. Bowel Dis. 18 (8) (2012) 1515–1522, https://doi.org/10.1002/ibd.21872.
[57] Y. Kamari, A. Shaish, S. Shemesh, E. Vax, I. Grosskopf, S. Dotan, D. Harats, Reduced atherosclerosis and inflammatory cytokines in apolipoprotein-E-deficient mice lacking bone marrow-derived interleukin-1α, Biochem. Biophys. Res. Commun. 405 (2) (2011) 197–203, https://doi.org/10.1016/j.bbrc.2011.01.008.
[58] S. Shemesh, Y. Kamari, A. Shaish, S. Olteanu, M. Kandel-Kfir, T. Almog, D. Harats, Interleukin-1 receptor type-1 in non-hematopoietic cells is the target for the pro-atherogenic effects of interleukin-1 in apoE-deficient mice, Atherosclerosis 222 (2) (2012) 329–336, https://doi.org/10.1016/j.atherosclerosis.2011.12.010.
[59] J.E. Hirshfeld-Cytron, F.E. Duncan, M. Xu, J.K. Jozefik, L.D. Shea, T.K. Woodruff, Animal age, weight and estrus cycle stage impact the quality of in vitro grown follicles, Hum. Reprod. 26 (9) (2011) 2473–2485, https://doi.org/10.1093/humrep/der183.
[60] L. Helming, S. Gordon, Molecular mediators of macrophage fusion, Trends Cell Biol. 19 (10) (2009) 514–522, https://doi.org/10.1016/j.tcb.2009.07.005.
[61] A.K. McNally, J.M. Anderson, Macrophage Fusion and Multinucleated Giant Cells of Inflammation, 2011, https://doi.org/10.1007/978-94-007-0763-4_7.
[62] L. Arruvito, A. Billordo, M. Capucchio, M.E. Prada, L. Fainboim, IL-6 trans-signaling and the frequency of CD4+FOXP3+ cells in women with reproductive failure, Journal of Reproductive Immunology 82 (2) (2009) 158–165, https://doi.org/10.1016/j.jri.2009.04.010.
[63] T. Shima, Y. Sasaki, M. Itoh, A. Nakashima, N. Ishii, K. Sugamura, S. Saito, Regulatory T cells are necessary for implantation and maintenance of early pregnancy but not late pregnancy in allogeneic mice, J. Reprod. Immunol. 85 (2) (2010) 121–129.
[64] K.T. Jones, S.I.R. Lane, Molecular causes of aneuploidy in mammalian eggs, Development 140 (18) (2013) 3719–3730, https://doi.org/10.1242/dev.090589.
[65] D. Liu, X. Tu, C. Huang, Y. Yuan, Y. Wang, X. Liu, W. He, Adoptive transfers of CD4 + CD25+ Tregs partially alleviate mouse premature ovarian insufficiency, Mol Reprod Dev. 87 (8) (2020) 887–898, https://doi.org/10.1002/mrd.23404.
[66] K. Song, H. Cai, D. Zhang, R. Huang, D. Sun, Y. He, Effects of human adipose-derived mesenchymal stem cells combined with estrogen on regulatory T cells in patients with premature ovarian insufficiency, Int. Immunol. 55 (2018) 257–262, https://doi.org/10.1016/j.intimp.2017.12.026.